Pulsating–gliding transition in the dynamics of levitating liquid nitrogen droplets

2008 New J. Phys. 10 043034

(http://iopscience.iop.org/1367-2630/10/4/043034)

New Journal of Physics
The open–access journal for physics

Pulsating–gliding transition in the dynamics of levitating liquid nitrogen droplets

Alexey Snezhko[1], **Eshel Ben Jacob**[2] **and Igor S Aranson**[1]
[1] Materials Science Division, Argonne National Laboratory,
9700 S Cass Avenue, Argonne, IL 60439, USA
[2] School of Physics and Astronomy, 69978 Tel Aviv University,
Tel Aviv, Israel
E-mail: aranson@msd.anl.gov

New Journal of Physics **10** (2008) 043034 (12pp)
Received 20 December 2007
Published 21 April 2008
Online at http://www.njp.org/
doi:10.1088/1367-2630/10/4/043034

Abstract. Hot surfaces can cause levitation of small liquid droplets if the temperature is kept above the Leidenfrost point (220 °C for water) due to the pressure formed because of rapid evaporation. Here, we demonstrate a new class of pulsating–gliding dynamic transitions in a special setting of the Leidenfrost effect at room temperatures and above a viscous fluid for droplets of liquid nitrogen. A whole range of highly dynamic patterns unfolds when droplets of liquid nitrogen are poured on the surface of another, more viscous liquid at room temperature. We also discovered that the levitating droplets induce vortex motion in the supporting viscous liquid. Depending on the viscosity of the supporting liquid, the nitrogen droplets either adopt an oscillating (pulsating) star-like shape with different azimuthal symmetries (from 2–9 petals) or glide on the surface with random trajectories. Thus, by varying the viscosity of the supporting liquid, we achieve controlled morphology and dynamics of Leidenfrost droplets.

Contents

1. Introduction	**2**
2. Droplet evaporation and convection	**3**
2.1. Evaporation rates	4
3. Dynamic behavior	**6**
3.1. Internal dynamics	6
3.2. Pulsating dynamics	6
3.3. Evaluation of number of petals and oscillation frequency	6
3.4. Gliding dynamics	9
4. Conclusions	**10**
Acknowledgments	**11**
Appendix. Estimation of the vapor layer thickness	**11**
References	**11**

1. Introduction

At temperatures above the *Leidenfrost point,* the bottom part of a water droplet evaporates immediately upon contact and the vapor pressure leads to levitation above the hot surface [1]. The vapor layer reduces heat transfer into the droplet, hence slows its evaporation so that it can continue to float for a long time. Friction also becomes reduced so the drop is able to skid around the pan on the layer of gas just under it like a toy puck skids above the surface of an air hockey table. Despite years of practical experience, many aspects of the rich dynamics of the levitating droplets under the Leidenfrost effect are still actively researched [2]–[7]. Previous studies, mostly focused on the behavior of droplets on rigid surfaces, have shown that the droplets exhibit rich dynamics with shape oscillations along the perimeter that cause them to appear as oscillating stars with different symmetries. The degree of symmetry (number of petals or arms) corresponds to the number of waves that fit along the perimeter. Wave propagation along the perimeter causes the droplet to appear as a rotating star—the arms look retracted and then extend at a new direction that is shifted by half a wavelength (see supplementary movie 1, available from stacks.iop.org/NJP/10/043034/mmedia) [5]–[7]. The horizontal dynamics of oscillations is coupled in vertical patterns of convection inside the droplet. The larger droplets exhibit higher degrees of symmetry. During the evaporation, the droplet slowly shrinks in diameter and transitions between dynamical modes of different degrees of symmetry are observed. Recently, with the development of fast digital video imaging techniques, the phenomenon gained renewed attention [3, 7].

In most previous studies the levitation was generated on hot and hard surfaces. It was also demonstrated for droplets of liquid nitrogen on hard curved surfaces [5, 7]. Here, we discovered that it is possible to generate levitation at room temperature and above the surfaces of viscous liquids. This technique has a number of advantages compared to the traditional Leidenfrost experiment. Firstly, the surface of the supporting liquid is perfectly smooth and level with respect to gravity, thus rendering such side effects as surface imperfections and small inclinations totally irrelevant. Consequently, our Leidenfrost droplets are typically more controllable and confined to a certain position given by the initial conditions compared to skidding droplets on flat hard surfaces. Secondly, evaporating droplets interact with the surface

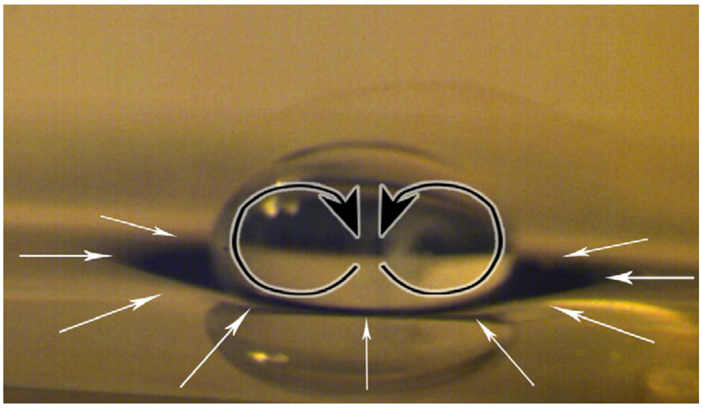

Figure 1. Liquid nitrogen droplet above the surface of glycerol at room temperature (side view). Arrows indicate toroidal vortex trajectories.

of the viscous liquid and generate nontrivial large-scale circulation in the bulk liquid. These large-scale flows, which obviously are sensitive to the viscosity, in turn affect the dynamics of the Leidenfrost effect in a highly nontrivial way. This new setting enabled us to study the effect of the surface viscosity on the levitation dynamics and to discover a new phenomenon—the transition from the pulsating state at high viscosity values to spontaneous gliding as the viscosity of the supporting liquid is reduced. In addition to the pulsating and gliding states, we also observed novel vertical, localized oscillating states occurring on the top cap of the droplet. The frequency of the droplet pulsation, estimated from simple arguments, is in good agreement with the experiment.

2. Droplet evaporation and convection

In our experiments, we deposited small droplets of liquid nitrogen on an initially calm surface made of viscous liquid (glycerol viscosity $\eta = 1.5\,\mathrm{Pa\,s}$, thermal conductivity $\kappa = 0.28\,\mathrm{W\,(m\,K)^{-1}}$, ethanol, viscosity $\eta = 1.2 \times 10^{-3}\,\mathrm{Pa\,s}$, thermal conductivity $\kappa = 0.18\,\mathrm{W\,(m\,K)^{-1}}$, toluene, or glycerol–ethanol mixture) at room temperature that is placed in a transparent 60 mm diameter Petri dish. Dynamic patterns were observed in the transmitted light using a high-speed digital camera, typical frame rate was 200 frames $\mathrm{s^{-1}}$. The recorded videos were then processed using image-processing software.

Figure 1 displays a side view of a levitating nitrogen droplet above the surface of glycerol. We observed that in the course of evaporation, strong toroidal vortex flows are generated in the droplet itself as well as in the bulk of the supporting liquid. While the vorticity generation in an evaporating droplet is anticipated (compare to vortices in evaporating water drops [8, 9]), the flow generation in the supporting liquid is rather surprising and has totally different nature. Figure 1 illustrates vortex flow directions (depicted by the arrows) in the nitrogen droplet (black arrows) due to evaporation processes, and on the surface of the supporting viscous liquid (glycerol), white arrows. The flow direction is extracted from the trajectories of tracers (e.g. ice micro crystals in liquid nitrogen, small air bubbles in glycerol). One notices that the evaporating nitrogen droplet induces strong converging flows on the surface and circulation in the bulk of the supporting liquid. Directions of the arrows, however, imply that the main mechanism leading to

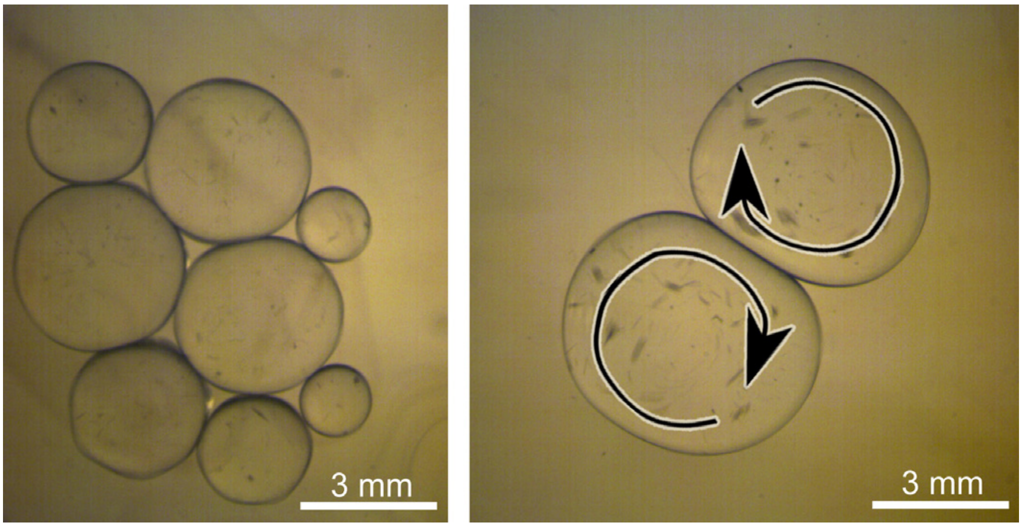

Figure 2. Multi-droplet bound states. Short-range repulsion between the droplets due to liquid nitrogen evaporation prevents immediate droplet coalescence. Right panel illustrates counter-rotating bound state of two Leidenfrost droplets, arrows show the direction of rotation, see supplementary movies 2 and 3, available from stacks.iop.org/NJP/10/043034/mmedia.

the appearance of these flows is associated with thermal convection induced by the temperature gradient between the droplet and the supporting liquid (cold liquid sinks down under the droplet) rather than by the nitrogen vapor flow drag (wind effect) of the evaporated droplet (that scenario would imply glycerol flow underneath the droplet in the reverse direction).

Multiple Leidenfrost droplets on the liquid substrate exhibit effective long-range attraction due to formation of a meniscus on the surface of the supporting liquid forcing the droplets to slide toward the center of the container. However, raising nitrogen vapor flows creates strong short-range repulsion, preventing immediate droplet coalescence and resulting in formation of long-living dynamic bound states as illustrated in figure 2 and supplementary movies 2 and 3 (available from stacks.iop.org/NJP/10/043034/mmedia).

2.1. Evaporation rates

The large-scale convective flows in the supporting liquid have a very strong effect on heat transfer, and, in turn, affect the evaporation rate of the droplet. In particular, due to this convection the supporting liquid cooled by the Leidenfrost droplet sinks, whereas warm liquid is sucked under the droplet, increasing the local temperature and accelerating evaporation. This particular mechanism of heat transfer is significantly affected by the viscosity of the liquid used to support the droplet: decreasing of the viscosity should intensify the convection and thus accelerate evaporation. In figure 3, the time evolution of a liquid nitrogen droplet is shown for different supporting liquids and compared with that for solid substrates with different thermal conductivities. In all cases, the evaporation dynamics agrees very well with the following scaling of droplet radius R with time t derived in [3]: $R = R_0(1 - t/\tau)^2$, where R_0 is initial droplet radius and τ is some constant. While the thermal conductivity of the liquids used in the experiment is low and does not change significantly from liquid to liquid (the range

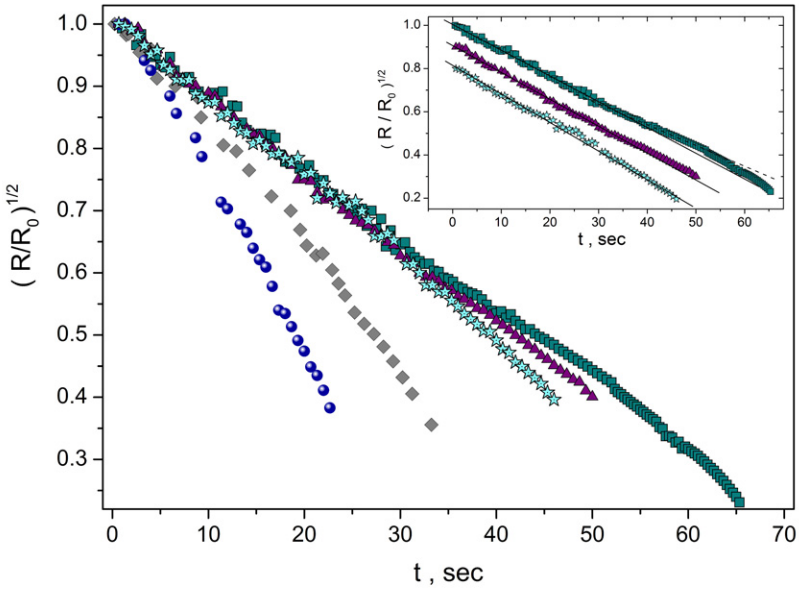

Figure 3. Time evolution of radius R of the liquid nitrogen droplet levitating above different types of substrate, R_0 is the initial radius of the droplet. The plots show $(R/R_0)^{1/2}$ versus time t as suggested in [3]. Droplet evaporation above the surface of liquids is presented for glycerol (squares), glycerol (76%)–ethanol (24%) mixture (triangles) and ethanol (diamonds). Solid substrates are represented by glass (stars) and copper (spheres). Inset: $(R/R_0)^{1/2}$ versus time curves for glycerol, glycerol–ethanol mixture and glass substrates were offset to demonstrate similarity in the evaporation rates during the first 30 s of evaporation. Solid curves are linear fits. Upturn of the curve for the case of glycerol is attributed to the effect of its high viscosity impeding heat transfer from the liquid to the nitrogen droplet (see text for details).

of values is from 0.18 W (m K)$^{-1}$ for ethanol to 0.28 W (m K)$^{-1}$ for glycerol) the viscosity experiences drastic changes—three orders of magnitude. As seen from figure 3, the evaporation rates are smallest in the case of glycerol (squares) and comparable to the case of liquid nitrogen droplet evaporation above a hard glass substrate (stars), which has three times higher thermal conductivity coefficient. In the first 30 s of the experiment the curves are quite indistinguishable. The subsequent slow down in the evaporation rate of the droplet above glycerol (upturn) is attributed to the fact that due to the high viscosity and low thermal conductivity of glycerol, the heat transfer from the surface of the liquid to the bulk slows down, leading to the formation of a ‘cold’ layer of glycerol beneath the nitrogen droplet. The cold layer in turn slows down the evaporation of the droplet: the temperature gradient between the droplet and the liquid is reduced. This upturn in the evaporation rate of the droplet could be tuned by the modification of the liquid’s viscosity. Addition of 24% of ethanol to glycerol reduces its viscosity by about 25%, however it makes the upturn feature of the evaporation rate much smaller, bringing the resulting curve (triangles) close to the glass case. In the extreme case of ethanol (diamonds), which has a viscosity more than 1000 times lower than that of glycerol, the process of evaporation is obviously much more effective compared to glycerol and considerably faster than that for glass, which has a thermal conductivity coefficient about 5 times higher than ethanol. The evaporation of the nitrogen droplet above the copper plate (that has more than 2000 times higher thermal conductivity than ethanol) is only slightly faster (spheres). All these results suggest that induced convective flows in the supporting liquid during the evaporation process of nitrogen droplets play an essential role in the heat transfer. Liquids with low thermal conductivity and viscosity can still be very efficient heat conductors similar to hard substrates with considerably higher thermal conductivity.

3. Dynamic behavior

3.1. Internal dynamics

The internal dynamics of the droplet deduced from the trajectories of dark particles (ice crystals) trapped in the droplet exhibits toroidal vortex flow; see figure 1, and supplementary movies 4 and 5 (available from stacks.iop.org/NJP/10/043034/mmedia). For a highly viscous liquid, such as glycerol, gravity deforms the glycerol surface under the droplet into a nest that traps it. However, the droplet oscillates, and surprisingly a localized splash-like object (by analogy we will call it an oscillon [10]) at the top cap of the droplet is often observed from the side (figure 4(b) and supplementary movie 4). The 'oscillons' typically oscillate with a frequency about four times faster than the droplet pulsations. In addition, due to the rapid vortex flow, the droplet surface undergoes a symmetry-breaking instability yielding a pair of counter-propagating waves similar to that described in [11, 12].

3.2. Pulsating dynamics

We observed that if liquid nitrogen is gently poured on the surface of a viscous liquid such as glycerol or silicon oil, the droplet rapidly turns into a multi-petal pulsating star-like structure (or pulsar) similar to that observed on hard surfaces [5]–[7], as shown in figure 4(a) (1–4) and supplementary movie 1. In addition to standing-wave type oscillations, some pulsars also rotate (figure 4(c) and supplementary movies 1 and 5). The number of petals N is determined roughly by the size of the droplet: in the course of evaporation there is a tendency toward reduction of N. The frequency of pulsar oscillations f is proportional to the effective wavenumber, $k = 2\pi/\lambda$, where λ is the distance between neighboring petals, see the main panel of figure 5. Figure 6 demonstrates an evolution of the number of petals as a function of time. As one can see, while there is an overall tendency towards the decrease of N, the dynamics is accompanied by nontrivial switching and oscillations of the number N reflecting complicated nonlinear competition between unstable surface deformation modes. Such nontrivial switching dynamics is a strong indication of simultaneous excitation and competition of multiple surface-deformation modes.

3.3. Evaluation of number of petals and oscillation frequency

In our experiment, the number of petals N and the oscillation frequency f depends on the radius of the droplet R. Similar shape instability is also observed in [13] for liquid droplets vibrated mechanically and for Leidenfrost droplets on rigid substrates. The number of petals $N = kR$, k is the wavenumber and is estimated from the frequency f and the phase velocity $v = 2\pi f/k$ of capillary waves, $v \approx (k\gamma/\rho)^{1/2}$, where $\gamma \approx 8\,\mathrm{dyn\,cm^{-1}}$ is the surface tension and

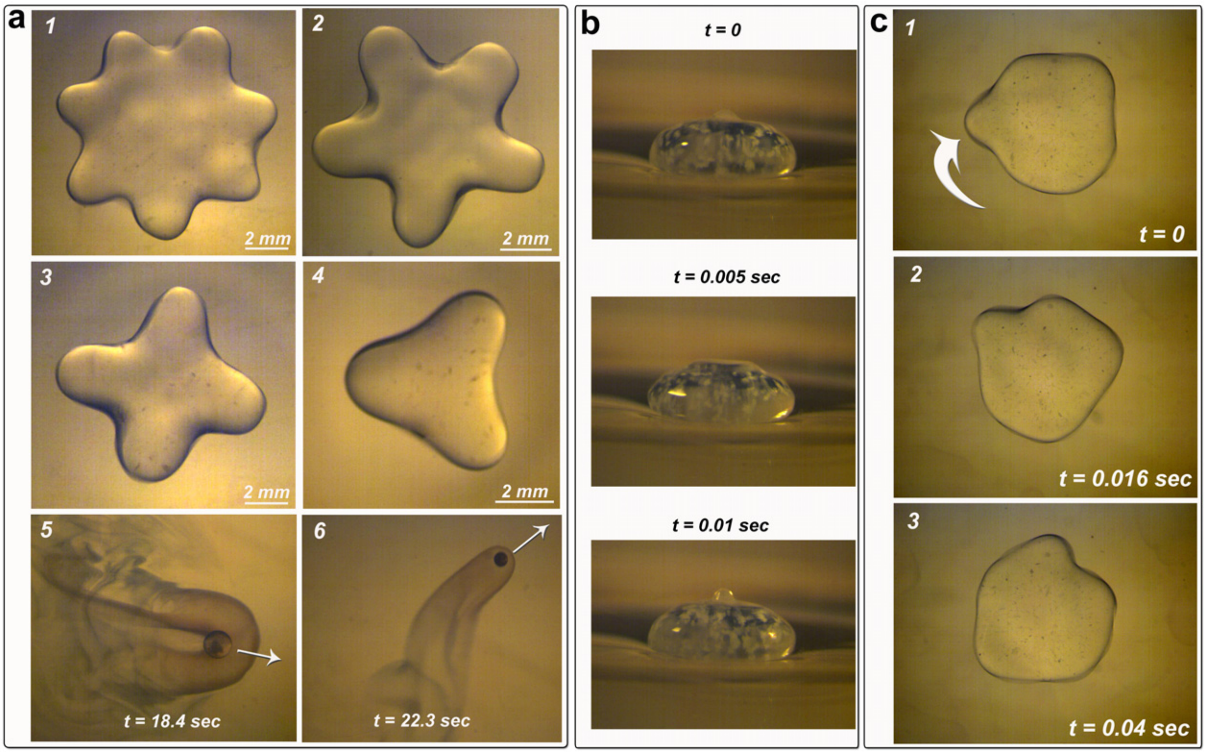

Figure 4. Liquid nitrogen droplet above the surfaces of liquids at room temperature. Panel a: images 1–4, nitrogen droplet oscillating on the surface of glycerol observed in transmission light. The number of petals in these pictures varies from 7 (image 1) to 3 (image 4). Gliding nitrogen droplets on the surface of toluene (comets) are shown in images 5 and 6. The comet's tail is formed by condensed vapor. Panel b: side view of vertical oscillations of the liquid nitrogen droplet. The panel shows oscillon formation in the center of the droplet. The frequency of the oscillon is about 110 Hz, which is almost four times faster than the horizontal oscillations of the droplet. Panel c: peak rotation on the droplet surface due to phase difference between running waves of opposite directions.

$\rho = 0.8\,\mathrm{g\,cm^{-3}}$ is the density of liquid nitrogen. Finally, we obtain the expression for the number of petals N and wavenumber k [6]

$$k = \frac{N}{R} = \left((2\pi f)^2 \frac{\rho}{\gamma}\right)^{1/3}, \tag{1}$$

which is in good agreement with the experimental observation, see figure 5.

Since the viscosity of the liquid nitrogen is relatively low, the frequency and the structure of surface modes are close to the Rayleigh frequency [14] of spherical inviscid droplets with the azimuthal number N:

$$f = \frac{1}{2\pi}\sqrt{\frac{\gamma(N-1)N(N+2)}{R^3\rho}}. \tag{2}$$

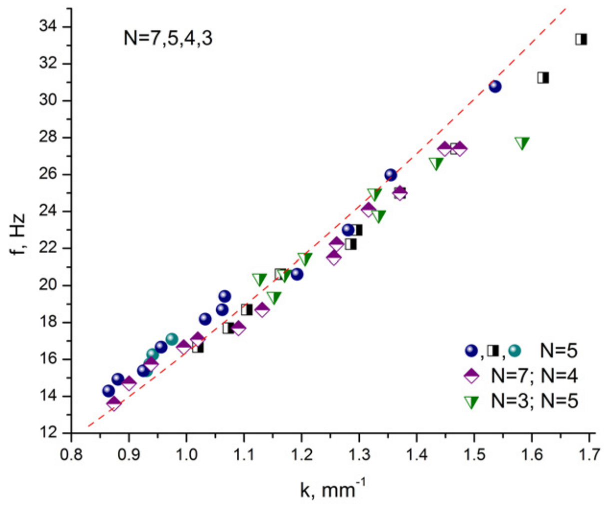

Figure 5. Frequency of pulsar oscillations versus wavenumber k; symbols correspond to different experiments, dashed curve visualizes the dispersion relation (1) for azimuthal surface oscillations (no fitting parameters).

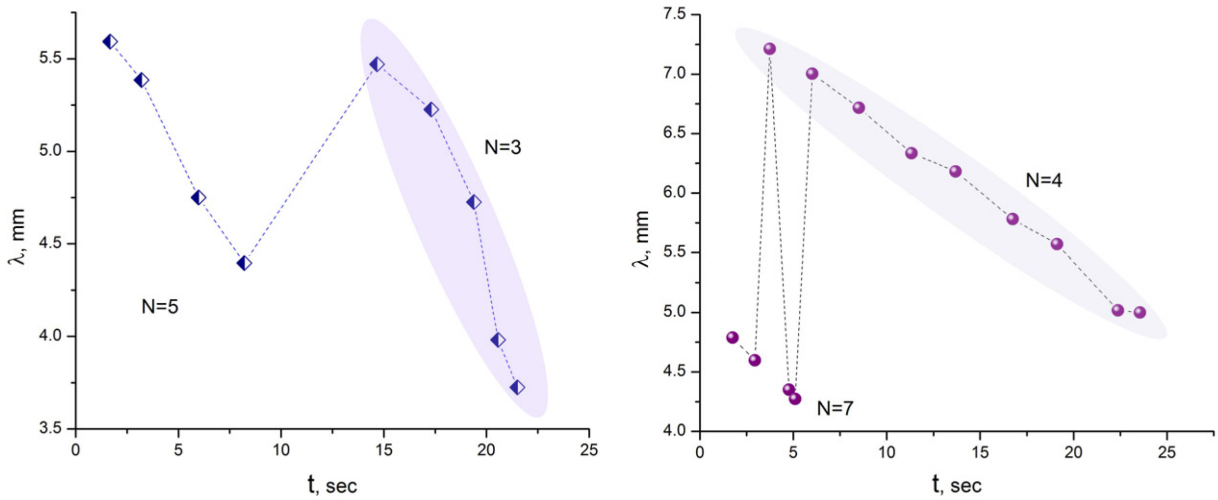

Figure 6. Time evolution of the number of petals in pulsars. Left panel: transition from 5- to 3-petal pulsar. Right panel: 7- to 4-petal pulsar evolution. The transition is determined by the volume of the droplet and appears to be hysteretic (7–4–7–4 transitions are indicative of the hysteretic behavior). The radius of the droplets decreased to half of the initial value during our experiments.

In [15], the corrected Rayleigh frequency for a droplet placed on a rigid substrate was derived as follows:

$$f = \frac{1}{2\pi}\sqrt{\frac{\gamma(N-1)N(N+2)}{R^3\rho\left(1+\sqrt{(2N+1)/4\pi}\right)}}. \tag{3}$$

Experimental dependences of the oscillation frequency f versus radius R for droplets with different numbers of petals N are shown in figure 7. Indeed, excellent agreement with equation (3) is observed.

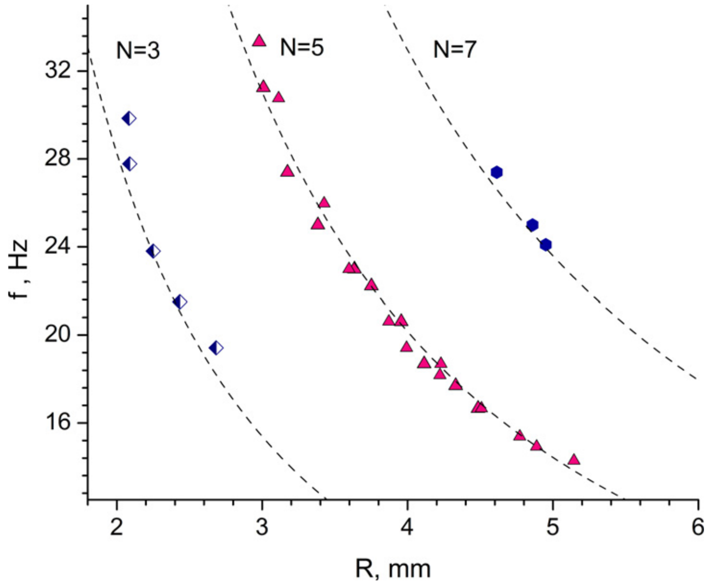

Figure 7. The pulsation frequency f of levitating nitrogen droplets on glycerol versus the effective droplet radius R plotted for the number of petals $N = 3$ (diamonds), 5 (triangles) and 7 (hexagons). Dashed lines show the solution to equation (3), no adjustable parameters were used.

3.4. Gliding dynamics

When placed on a less viscous liquid, such as toluene or ethanol (viscosity of toluene $\eta = 0.5 \times 10^{-3}$ Pa s is roughly 1000 times smaller than that of glycerol), the droplet motion is reminiscent of a rapidly moving comet, as it has a trail of vapor behind, see figures 4(a) (5 and 6) and supplementary movie 6. The droplet glides faster and faster during the course of evaporation. The velocity of the droplet rapidly increases with a reduction in its size; see figure 8. The velocity of gliding monotonically increases with decrease of the supporting liquid viscosity.

To explore the pulsating-to-gliding transitions, we mixed glycerol with ethanol in various proportions to alter the supporting liquid viscosity. For intermediate viscosities, a droplet may start as a pulsar and become a comet when its size is reduced. The transition from pulsating to gliding regime for the levitating nitrogen droplets occurs when the viscosity of the supporting liquid reaches values of roughly 0.5 Pa s. As discussed above, for a lower viscosity the Liedenfrost droplet generates strong convective flows in the supporting liquid, which in turn affects the evaporation dynamics. Consequently, the symmetry-breaking instability turns into translational asymmetry: the flow under the droplet surface alters the heat transfer rates so that the nitrogen evaporates with different rates on the opposite sides of the droplets, creating a kind of ‘steam engine’. Thus, the droplet is self-propelled and glides even without an imposed spatial gradient of surface energy [16]–[18], gradient of wettability [19], horizontal vibration [20], or heat gradient [4]. Typically, the droplet does not glide on a straight line trajectory: long ‘ballistic’ flights are mediated by abrupt stops and resumption of motion in a random new direction (see supplementary movie 6). We believe that this behavior might have the same underlying reason as the switching between various symmetry patterns illustrated in figure 4: due to competition

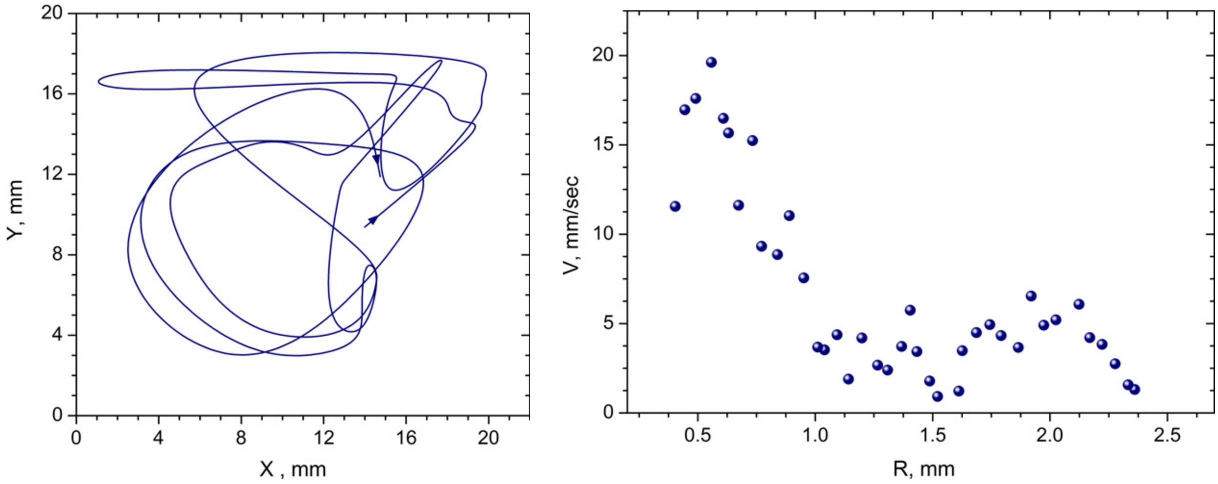

Figure 8. Left panel: typical trajectory of the center of a gliding Leidenfrost droplet (comet) on alcohol, see supplementary movie 6. Right panel: velocity of the droplet versus droplet size. The dips in the curve at $R \approx 1$ mm and $R \approx 1.5$ mm correspond to abrupt changes in the gliding direction of the self-propelled droplet.

between multiple surface modes, the position of the 'steam engine' of the droplet abruptly changes in the course of evaporation. While the droplet moves erratically (and even stops sometimes), there is a general trend of increasing droplet velocity with decreasing radius, see figure 8 (right panel).

4. Conclusions

We described a rich variety of dynamic phenomena occurring in a simple physical system: drops evaporating on the surface of a viscous liquid. Remarkably complex behavior is observed for multiple droplets on the surface of a liquid as well: depending on initial velocities and collision angles the droplets merge, bounce, or form long-lived dynamic bound states, see supplementary movies 2 and 3.

Our investigations complement the previous observations of nontrivial 'quantum-mechanical' behavior of oscillating droplets [21, 22] and illustrate the role of nonlinear competition between self-induced surface oscillations of the droplet and hydrodynamic flows in the supporting fluids. It is quite likely that gliding and oscillating Liedenfronst droplets will also exhibit some sort of 'quantum-mechanical' behavior similar to that of mechanically vibrated ones, intriguing questions that we leave for future studies.

Another important question is the intrinsic mechanism of vertical droplet oscillations and its relation to surface undulations. Tokugawa and Takaki [6] proposed a specific mechanism of the self-sustained oscillations caused by the dependence of surface tension due to contact with hot air at the periphery of the droplets. The theory, however, is based on a number of simplifying assumptions, e.g. it ignores the vortex flows in the droplet etc, and needs further experimental and theoretical validations. While accurate computer modeling of the observed phenomena in the framework of multiphase hydrodynamics might happen to be rather challenging, we anticipate that a somewhat similar phenomenological approach developed earlier for the description of the instability of toroidal vortices formed in electrostatically driven granular media can be applied with certain modifications [11, 12]. Our studies also illustrate the onset of the gliding behavior of Leidenfrost droplets caused by the intrinsic spontaneous symmetry-breaking transition in a pure homogeneous setting rather than the external temperature or the surface energy gradient. Further theoretical studies of the Liedenfrost effect on liquid surfaces using, for example, multi-phase computational fluid dynamics algorithms, are desperately needed.

Acknowledgments

This research was supported by the US DOE, grant # DE-AC02-06CH11357 at the Argonne National Laboratory and by the Tauber Funds at Tel Aviv University.

Appendix. Estimation of the vapor layer thickness

Following analysis of [3], the thickness of the nitrogen vapor layer e_0 for a flat liquid droplet can be estimated from the balance of the evaporation rate and the mass flow from the vaporized layer beneath the droplet:

$$e_0 = \left(\frac{3\eta\kappa\Delta T}{4L\rho_v\rho g a}\right)^{1/4} R^{1/2},$$

here, $L = 198\,\mathrm{kJ\,kg^{-1}}$ is the latent heat of evaporation, $\Delta T = 220\,\mathrm{K}$ is the temperature difference between the liquid nitrogen and the surface of the liquid, $\rho = 0.8\,\mathrm{g\,cm^{-3}}$ and $\rho_\mathrm{v} = 0.002\,\mathrm{g\,cm^{-3}}$ are the densities of liquid and gaseous nitrogen; $\eta = 1.14\times10^{-4}\,\mathrm{g\,cm\,s^{-1}}$, $\kappa = 1600\,\mathrm{erg\,K\,s\,cm^{-1}}$ are viscosity and thermal conductivity of gaseous nitrogen at mean temperature ($T = 210\,\mathrm{K}$), and $a = (\gamma/\rho g)^{1/4} \approx 0.2\,\mathrm{mm}$ is a capillary length, $\gamma \approx 8\,\mathrm{dyn\,cm^{-1}}$ is the surface tension of liquid nitrogen and g is the acceleration of gravity. The nitrogen data are taken from the NIST website http://webbook.nist.gov/chemistry/fluid/ for atmospheric pressure. For a droplet of radius $R = 0.5\,\mathrm{cm}$ one finds $e_0 \approx 0.15$–$0.18\,\mathrm{mm}$, which is similar to that of a water [3].

References

[1] Thimbleby H 1989 The Leidenfrost phenomenon *Phys. Educ.* **24** 300
[2] Quere D and Ajdari A 2006 *Nat. Mater.* **5** 429
[3] Biance A L, Clanet C and Quere D 2003 *Phys. Fluids* **15** 1632
[4] Linke H, Aleman B J, Melling L D, Taormina M J, Francis M J, Dow-Hygelund C C, Narayanan V, Taylor R P and Stout A 2006 *Phys. Rev. Lett.* **96** 154402
[5] Adachi K and Takaki R 1984 *J. Phys. Soc. Japan* **53** 4184
[6] Tokugawa N and Takaki R 1994 *J. Phys. Soc. Japan* **63** 1758
[7] Strier D E, Duarte A A, Ferrari H and Mindlin G B 2000 *Physica* A **283** 261
[8] Ristenpart W D, Kim P G, Domingues C, Wan J and Stone H A 2007 *Phys. Rev. Lett.* **99** 234502
[9] Deegan R D, Bakajin O, Dupont T F, Huber G, Nagel S R and Witten T A 1997 *Nature* **309** 827
[10] Umbanhowar P B, Melo F and Swinney H L 1996 *Nature* **382** 793
[11] Sapozhnikov M V, Tolmachev Y V, Aranson I S and Kwok W-K 2003 *Phys. Rev. Lett.* **90** 114301
[12] Aranson I S and Sapozhnikov M V 2004 *Phys. Rev. Lett.* **92** 234301

[13] Yoshiyasu N, Matsuda K and Takaki R 1996 *J. Phys. Soc. Japan* **65** 2068
[14] Rayleigh Lord 1879 *Proc. R. Soc. Lond.* **29** 71
[15] Courty S, Lagubeau G and Tixier T 2006 *Phys. Rev.* E **73** 045301
[16] Chaudhury M K and Whitesides G M 1992 *Science* **256** 1539
[17] Fisher L S and Golovin A A 2007 *Phys. Fluids* **19** 032101
[18] Sumino Y, Magome N, Hamada T and Yoshikawa K 2005 *Phys. Rev. Lett.* **94** 068301
[19] Daniel S, Sircar S, Gliem J and Chaudhury M K 2004 *Langmuir* **20** 4085
[20] Daniel S, Chaudhury M K and de Gennes P-G 2005 *Langmuir* **21** 4240
[21] Couder Y, Protiere S, Fort E and Boudaoud A 2005 *Nature* **437** 208
[22] Couder Y and Fort E 2006 *Phys. Rev. Lett.* **97** 154101